
PROJECT SUMMARY

Final Technical Report

**CRUSTAL STRUCTURE AND COMPOSITION
ALONG THE LARSE II PROFILE**

00HQGR0053

Christensen, N. and C.H. Thurber

Dept. of Geology and Geophysics, UW-Madison

1215 W. Dayton St., Madison, WI 53706

(608)262-4469 Fax: (608)262-6027

wlutter@geology.wisc.edu

Program Element – II

Key Words – Wave Propagation, Laboratory Studies

Research supported by the U.S. Geological Survey (USGS), Department of the Interior, under USGS award number 00HQGR0053. The views and conclusions contained in this document are those of the authors and should not be interpreted as necessarily representing the official policies, either expressed or implied, of the U.S. Government.

PROJECT SUMMARY

00HQGR0053

CRUSTAL STRUCTURE AND COMPOSITION ALONG THE LARSE II PROFILE

Christensen, N. and C.H. Thurber

Dept. of Geology and Geophysics, UW-Madison

1215 W. Dayton St., Madison, WI 53706

(608)262-4469 Fax: (608)262-6027

wlutter@geology.wisc.edu

Program Element – II

Key Words – Wave Propagation, Laboratory Studies

TECHNICAL ABSTRACT

In 1999, the U.S. Geological Survey and the Southern California Earthquake Center collected refraction and low-fold reflection data along a 150-km-long corridor extending from Santa Monica Bay northward to the western Mojave Desert. This profile was part of the second phase of the Los Angeles Region Seismic Experiment (LARSE II). Chief imaging targets include sedimentary basins beneath the San Fernando and Santa Clarita Valleys and the deep structure of major faults along the transect, including the Northridge, San Fernando, San Gabriel, and San Andreas faults. Tomographic modeling of first arrivals using the methods of Hole (1992) and Lutter (1999) produce velocity models that are similar to each other and are well resolved to depths of 5 to 7.5 km. These models, together with reflectivity suggest that the Cenozoic sedimentary basins underlying the San Fernando Valley and the northern Santa Clarita Valley (north of the San Gabriel fault) reach maximum depths of 5-6 km and 3.5-4.5 km, respectively. The western Mojave Desert (Antelope Valley) is also underlain by a prominent sedimentary basin with an interpreted maximum depth of 2.5-3.5 km. Velocities of "basement" rocks appear to average 5.75-6.0 km/s in the shallow crust beneath the Santa Monica Mts and the southern part of the central Transverse Ranges. In the northern part of the central Transverse Ranges, they are lower in velocity, 5.5-5.75 km/s. The San Andreas fault separates differing velocity structures between the central Transverse Ranges and the Mojave Desert, where relatively lower velocities in the Mojave Desert at shallow depths become relatively higher at 5 km depth. The San Andreas fault has a poorly constrained steep dip. A weak low-velocity zone beneath the southern Santa Susana Mts is centered approximately on the north-dipping aftershock zone of the 1971 San Fernando earthquake and may represent fracturing in the hanging wall of the San Fernando fault.

PROJECT SUMMARY

Non-Technical Summary

CRUSTAL STRUCTURE AND COMPOSITION ALONG THE LARSE II PROFILE

00HQGR0053

Christensen, N. and C.H. Thurber

Dept. of Geology and Geophysics, UW-Madison

1215 W. Dayton St., Madison, WI 53706

(608)262-4469 Fax: (608)262-6027

wlutter@geology.wisc.edu

Program Element – II

Key Words – Wave Propagation, Laboratory Studies

NON-TECHNICAL ABSTRACT

We have used 20,000 first-arrival travel-times to construct tomographic 2-D and 3-D velocity models along the main line of the 1999 Los Angeles Region Seismic Experiment (LARSE II) transect that image the upper 7.5-10 km of the crust. Our velocity models, along with reflectivity models and oil-well data, provide constraints on the depth and configuration of sedimentary basins imaged beneath the San Fernando, Santa Clarita, and Antelope Valleys. These images provide valuable static corrections for reflection processing and teleseismic studies, can provide velocity constraints for strong motion studies and can be used with laboratory rock measurements for interpretation.

INTRODUCTION

Southern California is a region of great earthquake hazard where determination of sedimentary basin structure and location of subsurface faults can provide important information for hazard mitigation. Two damaging earthquakes in the area of the San Fernando Valley, the 1971 M 6.7 San Fernando and the 1994 M 6.7 Northridge earthquakes, have motivated further efforts to image deep structure of the San Fernando Valley. To address these issues, Seventy-eight explosive sources were recorded by ~1000 receivers along the main line in this corridor (Line 2), which crosses, from south to north, the Santa Monica Mts, San Fernando Valley, Santa Susana Mts, Santa Clarita Valley, central Transverse Ranges, Mojave Desert, and Tehachapi Mts.

A similar experiment was conducted in 1994 (LARSE I) along a corridor through the east-central Los Angeles region, traversing the Los Angeles basin, San Gabriel Valley, San Gabriel Mountains, and Mojave Desert. Inverse and forward modeling of first arrivals (Lutter et al., 1999; Fuis et al., 2001) provided an image of velocity structure that when combined with oil-well data (Brocher et al., 1998), and laboratory rock-velocity measurements (McCaffree Pellerin and Christensen, 1998) has constrained interpretation of basin depth (Los Angeles and San Gabriel Valley basins), the geometry of the Sierra Madre fault at depth and the subsurface lateral extent of the Pelona schist. A study of reflectivity (Ryberg and Fuis, 1998; Fuis et al., 2001) has identified a gently north-dipping bright reflective layer in the mid-crust of the San Gabriel Mts. that is interpreted as a fracture zone containing fluids. This fracture zone is interpreted to be part of a decollement connecting the San Andreas fault with reverse faults to the south, including the Sierra Madre fault and the causative fault for the 1987 M 5.9 Whittier Narrows earthquake (Fuis et al., 2001).

In this study, we have produced 2-D velocity models based on inversion of first arrivals using damped least-squares and smoothing constraint inversion methods as described by Lutter et al. (1999). These models are resolved to depths of 5-7 km. In addition, we have used the tomographic algorithm of Hole (1992) to produce a 3-D velocity model for comparison. Reflectivity results (Fuis et al., in review) are compared with our velocity models in an effort to better establish the depths of sedimentary basins.

Our results from the modeling of active-source data from LARSE2 Line 2, supported by the USGS, have provided detailed images of the upper 7 km of the crust, in particular along the high-resolution segment traversing the San Gabriel Mountains. Our model provides valuable static corrections for reflection processing [Fuis et al., in review] and can be used with laboratory rock measurements for interpretation [McCaffree Pellerin and Christensen, 1998; Lutter et al., 1999].

GEOLOGIC SETTING

LARSE Line 2 (Figure 1) crosses the very complex geology of the western and central Transverse Ranges and the Mojave Desert. The western Transverse Ranges, including the Santa Monica Mts, San Fernando Valley, Santa Susana Mts, and eastern Ventura basin, are believed to have rotated more than 90 degrees clockwise since the lower Miocene from a position offshore of the Peninsular Ranges (Hornafius et al., 1986; Crouch and Suppe, 1993). The Santa Monica Mts, the southernmost range in this province, is an anticlinorium, exposing Mesozoic igneous and metamorphic rocks (Santa Monica Slate) in its core similar to rocks of the Peninsular Ranges (Dibblee, 1992; Crouch and Suppe, 1993). These rocks are overlain by Cenozoic clastic sedimentary and volcanic rocks that on the south are offset by gently dipping detachment faults. The whole anticlinorium is faulted on the south by the left-lateral/ reverse Malibu Coast-Santa

Monica-Hollywood fault system. The San Fernando Valley, to the north, is a Cenozoic sedimentary basin deposited on Mesozoic igneous and metamorphic rocks in the south and thrust beneath Cenozoic sedimentary rocks of the much deeper Ventura basin in the Santa Susana Mts on the north, (Winterer and Durham, 1954; Yeats 1987; Yeats et al., 1994). Basement depth determined from oil wells is 1.2-1.5 km in the south and more than 3 km in the north (Tsutsumi and Yeats, 1999). The San Gabriel fault (SGF), in the Santa Clarita Valley¹, north of the Santa Susana Mts, is an old branch of the San Andreas fault (SAF) that was active chiefly between 13 and 5 Ma, with offsets of 40-60 km (see summary in Powell, 1993). It separates rocks of the eastern Ventura basin on the southwest from rocks of the Ridge and Soledad basins on the northeast. The basins on either side of the SGF have quite different histories (Crowell, 1954, 1962, 1982; Jahns and Muehlberger, 1954; Winterer and Durham, 1954). Although the Ventura basin to the west extends to great depth, oil wells just southwest of the SGF penetrate a bedrock ridge at shallow depths of 0.5-3.0 km (Stitt, 1986; Yeats et al., 1994; Dibblee, 1996). The Ridge and Soledad basins are variously faulted and deposited on crystalline bedrock of the Central Transverse Ranges (central Transverse Ranges) to the north. These are echelon ranges underlain by Pelona Schist in the south and by Precambrian igneous and metamorphic rocks and Mesozoic igneous rocks in the north that have been offset 160 km along the SAF system from similar rocks in the San Bernardino Mts to the southeast (Matti et al., 1985; Meisling and Weldon, 1989). The Pelona Schist is separated from the Precambrian and Mesozoic rocks by a graben containing Cenozoic sedimentary rocks that is bounded on the south by the oldest branch of the SAF system, the San Francisquito fault (see Powell, 1993) and on the north by the Clearwater fault. The western Mojave Desert, or Antelope Valley, is underlain by a Cenozoic sedimentary basin as much as 2.5-3.5 km deep, with igneous and metamorphic rocks exposed on all sides, including a ridge adjacent to the SAF (Dibblee, 1967).

METHODS AND MODELING

Two-dimensional (2-D) iterative damped least-squares (DLS) and smoothing-constraint inversion (SCI) methods (Lutter et al., 1999) have been applied to approximately 20,000 first-arrival travel-times from 64 shots along Line 2. These shots range in charge size from 10-4000 lbs, providing usable recorded energy to at least 70 km for 25 percent of these shots and to 50 km for most shots. Model distances for the 2-D inversions were based on the radial distance from the southernmost shot, about 2 km from the coast. The average trend of Line 2 is 7.5 degrees east of north. Ray coverage extends to a depth of 10-15 km for all of the 2-D velocity models.

An initial set of coarse-grid DLS and SCI models were constructed to evaluate model resolution at depths >3-5 km where fine-grid models are poorly constrained and to provide starting models for a fine-grid model. Both the DLS and SCI models used a bicubic-spline parameterization (see Lutter et al., 1999 for details). A total of 372 velocity nodes were positioned in the coarse grid DLS model at a horizontal grid interval of 7.5 km. This model fit 7500 travel-times to an average RMS travel-time error of 62 ms. Diagonal resolution values >0.4 extend to a depth of 5-7.5 km. Segments of the final models (see figure 2) outside of this region (whitened model areas in figure 2) are poorly constrained for both coarse-grid (not shown) and fine-grid models. The corresponding coarse-grid SCI model at the same gridding fit the travel-time data to 65 ms and was used as a starting model for the fine-grid DLS inversion due to increased smoothness.

¹ "Santa Clarita Valley" is an informal name for the topographic basin surrounding the Santa Clara River in the vicinity of Saugus and Newhall, CA.

For the fine-grid DLS inversion model (Figure 2a), a total of 915 model parameters were positioned at a horizontal grid interval of 2.5 km. The vertical grid interval is 1 km at depths shallower than 2 km below sea level and increases to 2 km at greater depths. The fine-grid DLS model lowers the RMS error to 53 ms and resolves image detail to a depth of 3-4 km at a model distance range of approximately 10-110 km. Model details at greater depth do not change significantly from the coarse-grid DLS model. Consequently, we use the coarse-grid DLS model resolutions (> 0.4) as a better indicator of model of model reliability in the depth range, 4-8 km. An alternate fine-grid SCI model imaged comparable model detail and fit travel-time data to 47 ms. This model required 1818 parameters positioned at grid intervals twice as small as the coarse-grid_model intervals. We prefer the fine-grid DLS model (Figure 2a) as the final 2-D model due to superior resolution at depth.

Three-dimensional (3-D) velocity models were constructed using the method of Hole (1992) to evaluate artifacts from off-line geometry and to possibly improve delineation of near-surface detail. The grid-size dimensions formed a box 160 km long (approximately north-south) by 10 km wide (approximately east-west) by 32 km deep. Three sets of iterated inversions were performed using constant horizontal and vertical grid intervals per set. Grid interval values used were 2 km, 1 km, and 0.5 km respectively. The final model fits over 20,000 travel-times to an RMS error of 41 ms using 64 shots along Line 2 and also a well-coupled shot in the San Fernando Valley (shotpoint 9244) 5 km east of Line 2. The central slice from this 3-D velocity model (Fig. 2b) is aligned along Line 2. The geometry of shots and receivers for the Line 2 fall within a ± 2 km offset from the central slice.

MODEL INTERPRETATION AND RESULTS

The final 2-D and 3-D models are very similar in detail. Upper-crustal low-velocity regions (2-5 km/s) are located beneath the San Fernando, Santa Clarita, and Antelope Valleys, and high-velocity regions (>5 km/s) are located in the Tehachapi Mts, central Transverse Ranges, and the Santa Monica Mts (Fig. 2). A mid-crustal velocity contrast between the central Transverse Ranges and the Mojave Desert is located at model coordinate 70 km, below the surface of the SAF.

Resolution

The fine-grid DLS inversion model displayed in Figure 2a resolves model detail (horizontal grid interval of 2.5 km) to a depth of 3-4 km as indicated by the 0.4 contour value. At this grid interval only details south of the SAF are well resolved. However, model details especially within the sedimentary basins are no smaller than 5 km in horizontal extent. At depths $> 3-4$ km, the horizontal extent of model detail is on the order of 20-50 km. Model details are robust especially at depth as evidenced by the similarity of the coarse and fine-grid models (Figure 2a) and the 3-D model slice (Figure 2b). As diagonal resolutions for the 3-D velocity model are unavailable, we prefer to use diagonal resolutions from the coarse grid model (horizontal grid interval of 7.5 km) as an indicator of model reliability.

Interpretation

Our velocity models, along with reflectivity models and oil-well data, provide constraints on the depth and configuration of sedimentary basins along Line 2. The regions underlying the San Fernando, Santa Clarita, and Antelope Valleys have low velocities (2-5 km/s) and high velocity gradients (0.75/s-1.25/s) characteristic of Cenozoic sedimentary rocks in these locations (Stitt,

1986; Brocher et al., 1998; Tsutsumi and Yeats, 1999). The base of the regions of low velocity and high velocity gradient are described as follows: In the San Fernando Valley, this base slopes gently from ~1-km depth (depths given wrt sea level unless otherwise noted) in the Santa Monica Mts to ~5-km depth in the northern San Fernando Valley. In the Santa Clarita Valley, it slopes steeply southward from ~1-km depth on the south edge of the Sierra Pelona to ~3.5 km in the northern Santa Clarita Valley. In the Antelope Valley, it slopes moderately from the north side of the bedrock ridge just north of the SAF to ~3 km depth in the central Antelope Valley. On the north side of the Antelope Valley, it slopes gently southward from ~1-2 km depth at model coordinate 100 to the central Antelope Valley. These sloping boundaries generally correspond to velocity contours ranging from 5-5.5 km/s.

Zones of reflectivity can be seen in the vicinity of these sloping boundaries (Fig. 2, heavy white lines; Fuis et al., in review). These zones of reflectivity have finite widths, ~1 km, and are stacked reflections from offsets as large as 25 km--and hence wide angles. Without well penetrations, it is not possible to say exactly what these reflective zones represent--in particular, whether the bottoms or tops of these zones represent a change from Cenozoic sedimentary rocks to "basement". Unfortunately, the 2 basement-penetrating wells closest to Line 2, at 40 and 93 km model coordinates, are just beyond these reflective zones. The well at 40 km is south of the SGF, whereas the reflective zone in the northern Santa Clarita Valley terminates at the SGF (see Fuis et al., in review). The well at 93 km is in a region of velocity irregularity in the northern Antelope Valley, just north of the reflective zone there. Velocity logs are not available for either well, but they penetrate the 4-4.5 km/s velocity contours in our models. Note that the modeled depth of the reflective zone in the Mojave Desert, especially the northern Antelope Valley, is uncertain owing to low-fold of the reflection data.

Rock that has been penetrated by oil wells beneath the Cenozoic sedimentary rocks in all three valleys is igneous and metamorphic rock, except that Mesozoic sedimentary rock is penetrated in the western San Fernando Valley and in the Santa Susana Mts (Dibblee, 1967; Stitt, 1986; Brocher et al., 1998; Tsutsumi and Yeats, 1999). One well 6 km east of Line 2, in the southeastern San Fernando Valley, penetrated quartz diorite at 1.48 km from the surface (Brocher et al., 1998; Tsutsumi and Yeats, 1999). The sonic velocity of the quartz diorite increased from 4.5 to 5.00 km/s in the 70-m interval of this unit that was drilled, indicating that this basement rock type has a velocity greater than 5 km/s beneath the Cenozoic cover. Thus, it seems likely, in view of all the evidence presented above, that the reflective zones and correlative velocity and velocity-gradient changes in our models correspond to boundaries between Cenozoic sedimentary rocks and older basement rocks. In most cases, this basement rock is interpreted as igneous and (or) metamorphic rock, but in the northern San Fernando Valley, where low densities are observed (Langenheim et al., 2001), Mesozoic sedimentary rocks are also a possibility.

Through the areas of basement outcrop along Line 2, our models indicate surficial zones of high velocity gradient extending as deeply as 2 km. The zones are interpreted as regions of open cracks and weathering (see, e.g., McCaffree Pellerin and Christensen, 1998). Beneath this surficial zone in the Santa Monica Mts, basement rocks have velocities of 5.75-6.0 km/s, although this velocity is well resolved in only a small region. The Santa Monica Mts are underlain by Mesozoic granitic rocks and the Santa Monica Slate. Beneath this surficial zone of high velocity gradient in the central Transverse Ranges, basement rocks have velocities that average 5.75-6.0 km/s in the south part of the ranges and 5.5-5.75 km/s in the northern part. The south part of the ranges is underlain by Pelona Schist (between PF and SFF, Fig. 2); whereas the north part of the ranges is underlain by Precambrian igneous and metamorphic rocks and

Mesozoic igneous rocks (between CF and SAF, Fig. 2). Immediately north of the SAF, basement velocity beneath this surficial zone is 5.25-5.5 km/s, slightly lower than immediately south of the SAF (5.5-5.75 km/s). However at depths greater than 5 km, basement velocity is higher north of the SAF (5.75-6.00 km/s). Thus the SAF separates different velocity structures.

The subsurface extension of faults can be imaged in the velocity model (Figure 2) as tabular low-velocity zones or lateral velocity contrasts; these details must be interpreted in light of existing geologic and geophysical constraints (Lutter et al. 1999). Lateral velocity contrasts in the velocity images, especially the 3-D slice (Figure 2b), are consistent with an expected near-vertical dip for the SAF (see Fuis et al. 2001). A 5-km wide LVZ, positioned at the surface trace of the SAF is imaged in the upper 2 km of the DLS model (Figure 2a). The LVZ, less obvious in the central slice of the 3-D model (Figure 2b), is also observed in the slice positioned at 1 km offset (east) along the geometry of the LARSE II line adjacent to the SAF. At depth, velocity contours suggestive of a steep boundary between the contrasting basement types of the central Transverse Ranges and Mojave Desert are imaged in both models. However, resolution of this dip is poor. The Pelona fault, known to be a high-angle fault dipping toward the Soledad basin depocenter (Hendrix and Ingersoll, 1987), can be traced to just east of line 2. The Pelona fault in our models is imaged as a sharp lateral velocity gradient extending beneath Line 2. Finally, a north-dipping low-velocity zone beneath the southern Santa Susana Mts is centered on the aftershocks of the 1971 San Fernando earthquake and appears to lie above or north of the NHF (see Figure 2b). The NHF is interpreted by Tsutsumi and Yeats (1999) and Fuis et al. (in review) as the southward extension of the San Fernando fault. Thus, this low velocity zone may correlate with the hanging wall of the San Fernando fault. Perhaps the low velocities in this region arises from fracturing in the hanging wall; Fuis et al. (in review) show abundant faulting in this hanging wall from both the 1971 San Fernando and 1994 Northridge earthquakes.

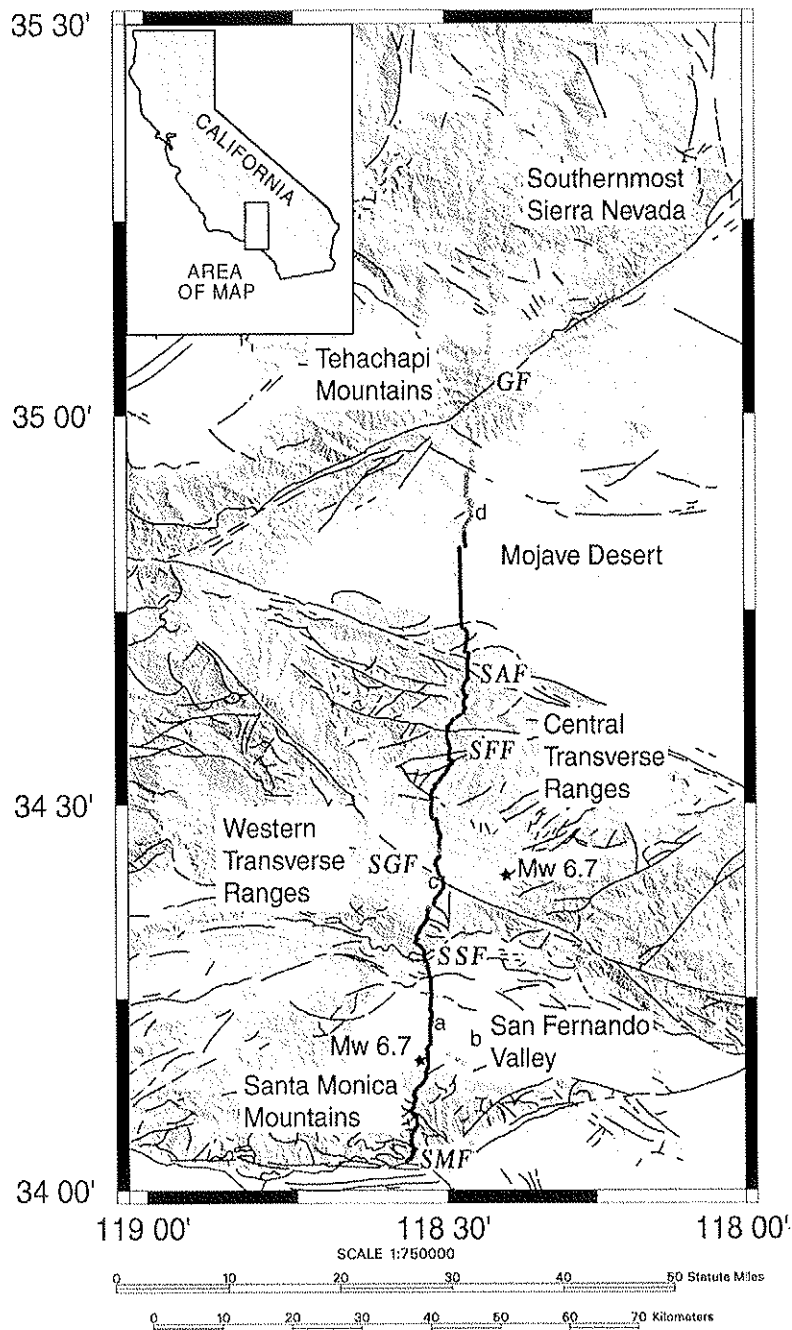


Figure 1. Fault map of part of southern California showing station positions along the main line of the 1999 LARSE II. The main line is 150 km long with shotpoint spacing ~1 km in the southern 80 km of the line and corresponding receiver spacing of 100 m. The northern part of the line was more sparsely shot and recorded. Stars indicate the positions of the 1971 M 6.7 San Fernando and 1994 M 6.7 Northridge earthquakes. Labeled faults are: SMF, Santa Monica fault; SSF, Santa Susana fault; SGF, San Gabriel fault; SFF, San Francisquito fault; SAF, San Andreas fault; GF, Garlock fault. Locations for oil wells are abbreviated a), Frieda J. Clark #1, Standard Oil of CA (Brocher et al., 1998); b), Leadwell #1, Standard Oil of CA (Brocher et al., 1998); c), Circle J #2, Mobil Oil Corp. (Stitt, 1986); and d), Meridian Oil (Dibblee, 1967).

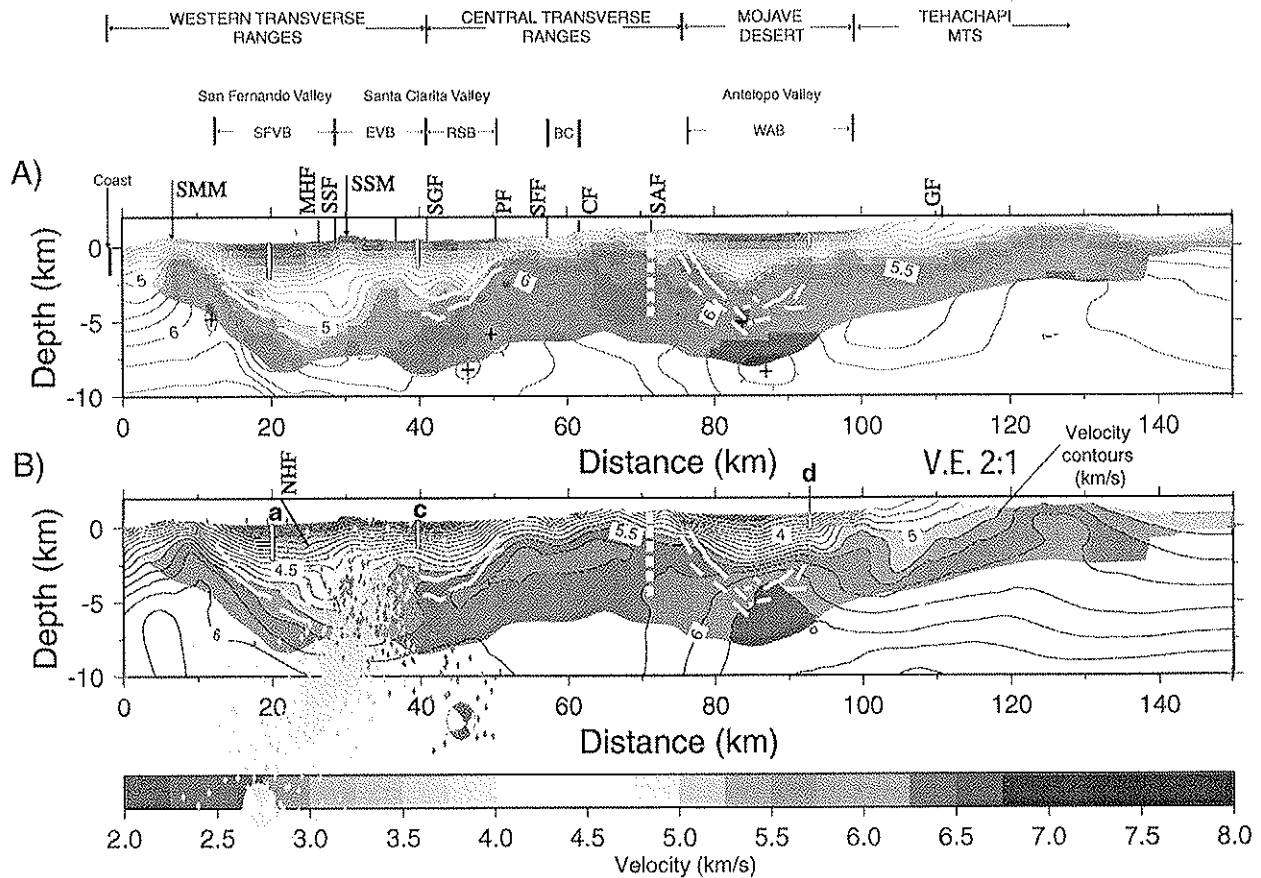


Figure 2. (A) Fine-grid DLS inversion model F1 (see Lutter et al., 1999) fits 7500 travel-times to an average RMS error of 53 ms. Faults are abbreviated as follows: SMF, Santa Monica fault; MHF, Mission Hills fault; NHF, Northridge Hills fault; SSF, Santa Susana thrust fault; SGF, San Gabriel fault; PF, Pelona fault; SFF, San Francisquito fault, CF, Clearwater fault; SAF, San Andreas fault; GF, Garlock fault. The Santa Monica Mts and Santa Susana Mts are abbreviated SMM and SSM respectively. The approximate subsurface extent of basins are identified as follows: SFVB, sedimentary basins within the San Fernando Valley; EVB, East Ventura basin; RSB, Ridge and Soledad basins (positioned west and east of the LARSE II main line, respectively); BC, Bee Canyon basin (subbasin of the Soledad basin); and the WAB, West Antelope basin. (B) 3-D velocity model (see Hole, 1992; lower panel displays central slice at 0 km offset from the 2-D model line) fits 20,000 travel-times to an RMS error of 41 ms. The solid white lines are tops and bottoms of zone of high reflectivity (Fuis et al., in review) interpreted to delineate the depth extent of basins. Lateral velocity contrasts and a near-surface LVZ positioned at a model distance of 70 km are consistent with a near-vertical dip for the SAF (see also Fuis et al., 2001, for dip of the SAF 80 km east). The Northridge (magenta) and San Fernando (red) earthquakes are superimposed, with focal mechanisms (vertically exaggerated) for the main shocks. These aftershocks are relocated using a tomographic velocity model of southern CA (Hauksson and Haas, 1997). The aftershocks plotted are within one month of the mainshocks and within 4 km of the LARSE II line. A diagonal resolution value of 0.4 from the coarse grid DLS model truncates the color definition of both models. White rectangles are oil test wells within 1-2 km of Line 2, with labels (see Figure 1) a) Frieda J. Clark #1 (bottoms in middle Miocene [Topanga] conglomerate), c) Circle J#2 (bottoms in "granite"), d) Meridian Oil (bottoms in quartz diorite).

PUBLICATIONS RESULTING FROM RESEARCH

- Lutter, W.J., G.S. Fuis, J.M. Murphy, D.A. Okaya, R.W. Clayton, P.M. Davis, N.J. Godfrey, T. Ryberg, C. Prodehl, G. Simila, G.R. Keller, H. Thybo, V.E. Langenheim, N.I. Christensen and C.H. Thurber (2000). Preliminary tomographic images from the Los Angeles Region Seismic Experiment, Phase II (LARSE II), Southern CA, (Fall Agu abstract), EOS Trans. AGU, 81, 2000.
- Lutter, W. J., G. S. Fuis, T. Ryberg, D.A. Okaya, R.W. Clayton, P.M. Davis, C. Prodehl, J.M. Murphy, M.L. Benthien, N.J. Godfrey, N.I. Christensen, K. Thygesen, C.H. Thurber, G. Simila, G.R. Keller, E. Hauksson, and V. Langenheim, Seismic Imaging of Basins and Faults along the Transect of the Los Angeles Regional Seismic Experiment, Phase 2 (LARSE II), In preparation for BSSA.

ADDITIONAL REFERENCES

- Brocher, T.M., A.L. Ruebel, T.L. Wright, and D.A. Okaya (1998). Compilation of 20 sonic and density logs from 12 oil test wells along LARSE Lines 1 and 2, Los Angeles region, California, U.S. Geological Survey Open-File Report 98-366, 53 p.
- Crouch, J.K., and J. Suppe (1993). Late Cenozoic evolution of the Los Angeles and inner California borderland: A model for core complex-like crustal extension, *Geol. Soc. Am. Bull.* **105**, 1415-1434.
- Crowell, J.C. (1954). Strike-slip displacement of the San Gabriel fault, Southern California, in *Geology of Southern California*, edited by Richard H. Jahns, California Division of Mines Bulletin 170, Chapter IV: Structural Features, v 1, pp. 49-52.
- Crowell, J.C. (1962). Displacement along the San Andreas fault, California, *Geol. Soc. Am. Spec. Pap.* **71**, 61 p.
- Crowell, J.C. (1982). The tectonics of the Ridge basin, southern California, in Crowell, J.C., and Link, M.H., eds., *Geologic History of the Ridge Basin, Southern California: Pacific Section*, Society of Economic Paleontologists and Mineralogists, p. 25-42.
- Dibblee, T.W., Jr. (1967). Areal geology of the western Mojave Desert, California: U.S. Geological Survey Professional Paper 522, 153 p.
- Dibblee, T.W., Jr. (1992). Geologic map of the Topanga and Canoga Park (south 1/2) quadrangles, Los Angeles County, California: Santa Barbara, Calif., Dibblee Geological Foundation, scale 1:24000.
- Dibblee, T.W., Jr. (1996). Geologic map of the Newhall quadrangle, Los Angeles County, California: Santa Barbara, Calif., Dibblee Geological Foundation, scale 1:24000.
- Fuis, G.S., R.W. Clayton, P.M. Davis, T. Ryberg, W.J. Lutter, D.A. Okaya, J.M. Murphy, M.L. Benthien, S.A. Baher, M.D. Kohler, K. Thygesen, G. Simila, G.R. Keller, E. Hauksson, K.B. Richards-Dinger (2002). Structure of the Northridge, San Fernando, and related faults along the LARSE II transect, southern California: A deep connection to the San Andreas fault, submitted to *Geology*.
- Fuis, G.S., Murphy, J.M., Okaya, D.A., Clayton, R.W., Davis, P.M., Thygesen, K., Baher, S.A., Ryberg, T., Benthien, M.L., Simila, G., Perron, J.T., Yong, A.K., Reusser, L., Lutter, W.J., Kaip, G., Fort, M.D., Asudeh, I., Sell, R., Vanschaack, J.R., Criley, E.E., Kaderabek, R., Kohler, W.M., Magnuski, N.H. (2001a). Report for borehole explosion data acquired in the 1999 Los Angeles Region Seismic Experiment (Larse II), southern California: Part I, description of the survey: U.S. Geological Survey Open-File Report 01-408, 86 p.

- Fuis, G.S., T. Ryberg, N.J. Godfrey, D.A. Okaya, and J.M. Murphy (2001). Crustal structure and tectonics from the Los Angeles basin to the Mojave Desert, southern California, *Geology* **29**, 15-18.
- Hauksson, E., and J.S. Haas (1997). Three-dimensional Vp and Vp/Vs Velocity Models of the Los Angeles basin and central Transverse Ranges, California, *J. Geophys. Res.* **102**, 5423-5453.
- Hendrix, E.D., and R.V. Ingersoll (1987). Tectonics and alluvial sedimentation of the upper Oligocene/lower Miocene Vasquez Formation, Soledad basin, southern California, *Geol. Soc. Am. Bull.* **98**, 647-663.
- Hole, J. (1992). Nonlinear High-Resolution Three-Dimensional Seismic Travel Time Tomography, *J. Geophys. Res.* **97**, 6553-6562.
- Hornafius, J.S., Luyendyk, B.P., Terres, R.R., and Kamerling, M.J. (1986). Timing and extent of Neogene tectonic rotation in the western Transverse Ranges, California, *Geol. Soc. Am. Bull.* **97**, 1476-1487.
- Jahns, R.H., and W.R. Muehlberger (1954). Geology of Soledad basin, Los Angeles county, in *Geology of Southern California*, edited by Richard H. Jahns, California Division of Mines Bulletin 170, v 2, Map sheet no. 6.
- Langenheim, V.E., T.G. Hildenbrand, R.C. Jachens, and A. Griscorn (2001). Geophysical setting of the San Fernando Basin, southern California, in Wright, T.L., and Yeats, R.S., eds., *Geology and Tectonics of the San Fernando Valley and East Ventura Basin*: Am. Assoc. of Petr. Geol., Pacific Section, GB77, p. 37-54.
- Lutter, W. J., G. S. Fuis, C. H. Thurber, and J. R. Murphy (1999). Tomographic images of the upper crust from the Los Angeles Basin to the Mojave Desert, California: Results from the Los Angeles Region Seismic Experiment, *J. Geophys. Res.*, **104**, 25,543-25,565.
- Matti, J.C., D.M. Morton, and B.F. Cox (1985). Distribution and geologic relations of fault systems in the vicinity of the central Transverse Ranges, southern California: U.S. Geological Survey Open-File Report 85-365, 27 p. scale 1:250,000.
- McCaffree Pellerin, C.L., and N.I. Christensen (1998). Interpretation of crustal seismic velocities in the San Gabriel-Mojave Region, southern California, *Tectonophysics* **286**, 253-271.
- Meisling, K.E., and R.J. Weldon (1989). Late Cenozoic Tectonics of the Northwestern San Bernardino Mountains, southern California, *Geol. Soc. Am. Bull.* **101**, 106-128.
- Powell, R.E. (1993). Balanced Palinspastic Reconstruction of Pre-Late Cenozoic Paleogeology, Southern California: Geologic and Kinematic Constraints on Evolution of the San Andreas Fault System, in *The San Andreas Fault System: Displacement, Palinspastic Reconstruction, and Geologic Evolution*, edited by R. Powell, R. Weldon, II, and J. Matti, *Geol. Soc. Am. Memoir* **178**, p. 1-106.
- Ryberg, T., and G.S. Fuis (1998). The San Gabriel Mountains bright reflective zone: Possible evidence of young mid-crustal thrust faulting in southern California, *Tectonophysics*, **286**, 31-46.
- Stitt, L.T. (1986). Structural history of the San Gabriel fault and other Neogene structures of the central Transverse Ranges, in *Neotectonics and Faulting in Southern California*, compiled by P.L. Ehlig: Geological Society of America, 82nd Annual Meeting of Cordilleran Section, Guidebook and Volume for Field Trips 10, 12, 18, p. 43-102.
- Tsutsumi, H., and R.S. Yeats (1999). Tectonic setting of the 1971 Sylmar and 1994 Northridge earthquakes in the San Fernando Valley, California, *Bull. Seismol. Soc. Am.* **89**, 1232-1249.

- Winterer, E.L., and D.L. Durham (1954). Geology of a part of the eastern Ventura basin, Los Angeles county, in *Geology of Southern California*, edited by Richard H. Jahns, California Division of Mines Bulletin 170, v 2, Map sheet no. 5.
- Yeats, R.F. (1987). Late Cenozoic structure of the Santa Susana fault zone, *U.S. Geol. Surv. Prof. Pap.* **1339**, 137-160, 1pl..
- Yeats, R.S., G.J. Huftile, and L.T. Stitt (1994). Late Cenozoic tectonics of the east Ventura basin, Transverse Ranges, California, *AAPG Bulletin* **78**, 1040-1074.

FIGURE CAPTIONS

Figure 1. Fault map of part of southern California showing station positions along the main line of the 1999 LARSE II. The main line is 150 km long with shotpoint spacing ~1 km in the southern 80 km of the line and corresponding receiver spacing of 100 m. The northern part of the line was more sparsely shot and recorded. Stars indicate the positions of the 1971 M 6.7 San Fernando and 1994 M 6.7 Northridge earthquakes. Labeled faults are: SMF, Santa Monica fault; SSF, Santa Susana fault; SGF, San Gabriel fault; SFF, San Francisquito fault; SAF, San Andreas fault; GF, Garlock fault. Locations for oil wells are abbreviated a), Frieda J. Clark #1, Standard Oil of CA (Brocher et al., 1998); b), Leadwell #1, Standard Oil of CA (Brocher et al., 1998); c), Circle J #2, Mobil Oil Corp. (Stitt, 1986); and d), Meridian Oil (Dibblee, 1967).

Figure 2. (A) Fine-grid DLS inversion model F1 (see Lutter et al., 1999) fits 7500 travel-times to an average RMS error of 53 ms. Faults are abbreviated as follows: SMF, Santa Monica fault; MHF, Mission Hills fault; NHF, Northridge Hills fault; SSF, Santa Susana thrust fault; SGF, San Gabriel fault; PF, Pelona fault; SFF, San Francisquito fault; CF, Clearwater fault; SAF, San Andreas fault; GF, Garlock fault. The Santa Monica Mts and Santa Susana Mts are abbreviated SMM and SSM respectively. The approximate subsurface extent of basins are identified as follows: SFVB, sedimentary basins within the San Fernando Valley; EVB, East Ventura basin; RSB, Ridge and Soledad basins (positioned west and east of the LARSE II main line, respectively); BC, Bee Canyon basin (subbasin of the Soledad basin); and the WAB, West Antelope basin. (B) 3-D velocity model (see Hole, 1992; lower panel displays central slice at 0 km offset from the 2-D model line) fits 20,000 travel-times to an RMS error of 41 ms. The solid white lines are tops and bottoms of zone of high reflectivity (Fuis et al., in review) interpreted to delineate the depth extent of basins. Lateral velocity contrasts and a near-surface LVZ positioned at a model distance of 70 km are consistent with a near-vertical dip for the SAF (see also Fuis et al., 2001, for dip of the SAF 80 km east). The Northridge (magenta) and San Fernando (red) earthquakes are superimposed, with focal mechanisms (vertically exaggerated) for the main shocks. These aftershocks are relocated using a tomographic velocity model of southern CA (Hauksson and Haas, 1997). The aftershocks plotted are within one month of the mainshocks and within 4 km of the LARSE II line. A diagonal resolution value of 0.4 from the coarse grid DLS model truncates the color definition of both models. White rectangles are oil test wells within 1-2 km of Line 2, with labels (see Figure 1) a) Frieda J. Clark #1 (bottoms in middle Miocene [Topanga] conglomerate), c) Circle J#2 (bottoms in "granite"), d) Meridian Oil (bottoms in quartz diorite).